2008 IEEE International Conference on
Robotics and Automation
Pasadena, CA, USA, May 19-23, 2008

Design of a Robot Joint with Variable Stiffness

Junho Choi, Sunchul Park, Woosub Lee, and Sung-Chul Kang

Abstract— **A robot joint with a variable stiffness unit is presented. The variable stiffness unit (VSU) is composed of a motor, two rings that consist of arc-shaped magnets separated by spacers, and a linear guide to change the cross-sectional area of the two rings. Angular displacement between two rings causes the magnets to generate torque, which acts as a nonlinear spring. The stiffness of the joint is varied via changing the overlapping area of the magnets. The VSJ exhibits nearly zero stiffness, which enables robot manipulator to be harmless to humans at a wide range of operating speed. Connected to a joint motor in series, the stiffness by the VSU and the position of the joint are controlled independently by two motors. The torque generated by the magnets is analyzed. Using dynamics of the joint, feedback linearization method is adopted to control the VSJ. In addition to feedback linearization, an integral controller is augmented in order to reduce the effect of model uncertainty and disturbances.**

I. INTRODUCTION

A service robot often shares its working space with humans, which increases the possibility of unexpected collision with humans. Therefore, in designing service robots, it is primary concerns for the robots to remain safe even in unexpected collisions. Introducing compliance at joints of manipulator provides a solution for enhancing the physical safety. However, a robot with compliant joints poses various problems, including stability and control. In [1], a robot with rigid joints was controlled to exhibit compliant motion using force feedback. Zinn *et al.* used parallel actuation using two motors with different characteristics [2]. A large actuator was used for high-torque and low-frequency movement, while low-torque and high-frequency movement was covered by a small actuator. In order to reduce inertia of the manipulator, the large motor was located in the base of the manipulator and the small motor was place at the joint.

Active compliance is more flexible in realizing it but it may be unreliable due to sensor failure and limited by sampling frequency, which was pointed out by Wang *et al.* in [3], where a comparison study was conducted. Since active compliance is limited in ensuring the manipulator to remain safe, passive compliance has been paid attention due to its reliability when safety is primary concern. Bicchi *et al.* investigated a robot joint with nonlinear springs and the control problem associated with the mechanical compliance in [4]. In [5], Tonietti *et al.* suggested variable stiffness actuation approach. Compliance was realized by two motors that were connected with a timing belt to a link. The mean of the positions of two motors becomes the position of the link while the generated stiffness was a function of relative position of two motors. Morita and Sugano developed a robot joint with a mechanical impedance adjuster in [6]. A leaf spring was adopted to a robot finger for soft grasping. The stiffness of the spring was adjusted by moving the pivot point. In [7], [8], a human shoulder was imitated by a 3-DOF mechanism that has programmable passive compliance. Yoon *et al.* introduced a robot manipulator with MR-based compliance for a service robot [9]. The robot manipulator was equipped with a rotary spring and a magneto-rheological (MR) rotary damper to reduce the vibration from the spring.

The control problem due to compliance has been addressed by many researchers. Spong used a static feedback linearization to control a robot manipulator with elastic joints in [10]. Dynamic non-linear state-feedback linearization was studied to control robots with elastic joints [11], [12].

In this paper, a robot joint with a Variable Stiffness Unit (VSU) is studied. The VSU consists of two concentric rings. Each ring is composed of four arc-shaped magnets and four arc-shaped spacers. The poles of magnets in each ring alternates so that relative angular displacement between the rings generates torque. The stiffness is varied by changing the overlapping area of the rings. The torque generated by the magnets is analyzed and feedback linearizing controller is used. Developed VSJ is designed for a manipulator with proximity sensing capabilities to avoid unexpected collision before the collision. The VSU is for preventing the manipulator from damaging humans when the proximity sensing is failed and collision occurs. When unexpected collision occurs, the VSU absorbs the initial impact from the collision. After the VSU absorbing the initial impact, the joint rotates to avoid further damage to the humans. The Head Injury Criteria (HIC) suggested by Versace in [13] is used to predict seriousness of the damage caused by the manipulator.

II. DESIGN OF THE VSJ

In this section, the design of the variable stiffness joint (VSJ) is explained. The principles of generating torque using permanent magnets and changing the torque are explained and explanation on mechanical system follows.

A. Realizing variable stiffness using permanent magnets

The VSU has two concentric rings with different radii sharing a common rotational axis. Each ring is composed of four arc-shaped magnets and four arc-shaped spacers. Each magnet is magnetized in the radial direction. The spacers are not magnetized. The magnets are arranged so that the direction of magnetization alternates, see Fig. 1. The inner ring is called "Rotor" and the outer ring is called "Stator."

Authors are with Center for cognitive robotics research, Korea Institute of Science and Technology, Seoul, Korea {junhochoi,hoodtman,robot,kasch}@kist.re.kr

Since two magnets with the same poles generate repulsive

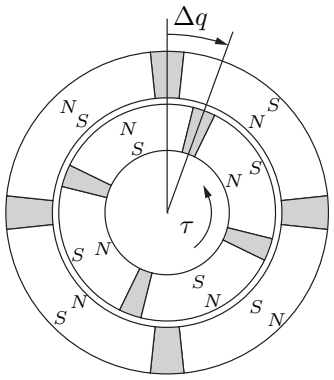

Fig. 1. Two concentric ring composed of magnets. Two adjacent magnets are magnetized in the opposite direction. Gray parts between the magnets are spacers, which are not magnetized. Δq is displacement from the neutral position. τ is the torque generated by the magnets.

force and attractive force is generated between magnets with an opposite poles, the VSU is in neutral position when each magnet of the rotor faces with a magnet with opposite pole of the stator. When external torque is applied, either the rotor or the stator rotates away from the neutral position. Due to the relative angular displacement, Δq, and the magnetic field between the rotor and the stator, torque counteracting to the external torque is generated, which acts as a nonlinear spring. Since four magnets are used in each ring, there are two stable neutral positions, which implies the angular displacement is limited to $-\frac{\pi}{2} < \Delta q < \frac{\pi}{2}$ in order to act as a spring. When the angular displacement exceeds the limit, the joint rotates to the other stable neutral position, which could cause injury to humans. Therefore, it is necessary to design frames to guarantee the angular displacement does not exceeds the limit.

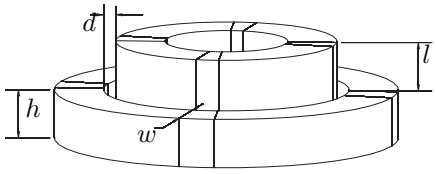

Fig. 2. Stiffness is changed by displace in axial direction.

Using analysis of [14] and neglecting the effect of the fringe magnetic flux, the generated torque is given as

$$\tau = L \sum_m c_1(m) \sin(c_2(m)\Delta q), \tag{1}$$

where L is the height of the overlapping area, $c_1(m)$ and $c_2(m)$ are constants determined from the dimension of the rings and materials of the magnets. $c_1(m)$ converges to 0 as m goes to ∞. Then, the generated torque is approximated to

$$\tau \approx cL\Delta q. \tag{2}$$

Since the generated torque is a function of the height of the overlapping area, the torque is varied when either the rotor or stator moves in the axial direction with the angular displacement unchanged, see Fig. 2.

Note that the neutral position in the axial direction is when the overlapping area becomes maximum. Assuming no fringe magnetic flux, the overlapping area becomes zero when $h - l$ becomes zero, which implies no torque is generated with nonzero angular displacement. Since angular displacement does not affect the torque generated, the dynamics of the joint motor and the stator is decoupled with the dynamics of the link and the rotor. Therefore, the effective inertia is reduced. Reduced effective inertia implies that higher operating speed of the link is allowed while the link remains safe to humans.

B. Variable Stiffness Joint (VSJ)

A motor for joint actuation, which is called "Joint motor", is attached to a frame. The frame holds a linear guide, whose lead screw is connected to another motor called "VSU motor." The stator is attached to the nut of the lead screw and the rotor is connected to the link. Since the stator is attached to the nut of the lead screw, the stator moves in the axial direction of the lead screw. Rotation of the stator is not allowed. On the contrary, the rotor is allowed to rotate only.

The stiffness and the position are controlled independently. Except for possible friction between the link and the frame, the rotor does not have any physical contact with the stator or the frame.

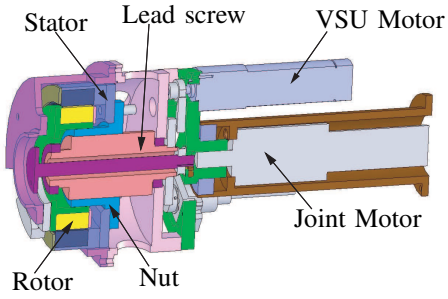

Fig. 3. A variable stiffness joint. It consists of the joint motor, two concentric rings composed of arc-shaped magnets and spacers, and a linear guide to make displacement.

III. Head Injury Criteria (HIC)

In this section, the Head Injury Criteria (HIC) suggested in [13] is explained. The HIC was designed to measure the damage caused in an car accident. It was derived via experiment on animals and human cadavers. It is adopted to measure the seriousness of damage caused by the joint in various literatures [15], [16].

Let T represent the time duration of the impact. Let $a(\zeta)$ is the acceleration of an object that collides with the link. Note that the acceleration is in unit of g not m/s^2. Then the HIC is given as follows.

$$\text{HIC} = T \left(\frac{1}{T} \int_0^T a(\zeta)\, d\zeta \right)^{2.5}, \tag{3}$$

which implies the value of the HIC changes as the time duration of the impact. The time duration of the impact is defined such that the HIC value becomes the maximum. The value of the HIC for general robot manipulator is obtained by either simulations or experiments.

The HIC is to indicate whether the damage caused by an impact is fatal or not. Since the HIC does not indicate how serious the damage is, the Expanded Prasad/Mertz curves are used to calculate the probability of serious injury using the HIC [17]. According to the Expanded Prasad/Mertz curves, the HIC being less than 100 means more than 92% of impacts results in no damage to the humans while less than 1% causes serious damages.

In order for the joint to remain safe during operation, the HIC needs to be less than maximum allowable value, which is achievable with either lower stiffness or lower operating speed. Lower stiffness allows the robot to operate at higher speed, which implies satisfying the safety condition without degrading performance. Note that the HIC value is proportional to the ratio of the manipulator to the mass of the object. The heavier the manipulator is, the more dangerous it becomes.

IV. Simulation and Experiment

In this section, results of experiments to evaluate properties of the implemented VSJ are presented.

Fig. 4 is the picture of the implemented VSJ. It consists of the VSU and the joint motor. The angular displacement between the rotor and the stator is measured by an absolute encoder. Position of the shaft of each motor is measured by an incremental encoder attached to the shaft.

Fig. 4. Implemented VSJ. It consists of two motors and VSU.

The parameters for the VSJ are shown in Table I. J_s represents the inertia of the stator, which includes the inertia of the motor rotor and the gear located between the stator and the motor. J_r denotes the inertia of the rotor. The VSJ is designed to use additional gear in order to satisfy the payload requirement. The gear ratio is set to be 9 to 1.

Parameters	unit	Value	Parameters	unit	Value
Mass	(kg)	5.2	J_s	kgm^2	7.7×10^{-3}
Diameter	(m)	0.15	J_r	kgm^2	1.0×10^{-3}
height	(m)	0.23			

TABLE I
MODEL PARAMETERS FOR THE VSU

Fig. 5 shows the torque generated by the VSU as the angular displacement varies. The VSU generates the torque proportional to the angular displacement with the angular displacement up to $20°$. When the angular displacement is less than $20°$, each stiffness $\sigma = \frac{\partial \tau}{\partial \Delta q}$ is approximated to a constant. The experimental result shows that the maximum stiffness is approximately $49.4Nm/rad$ and the minimum stiffness is $4.08Nm/rad$. When the angular displacement is larger than $20°$, the stiffness becomes almost zero.

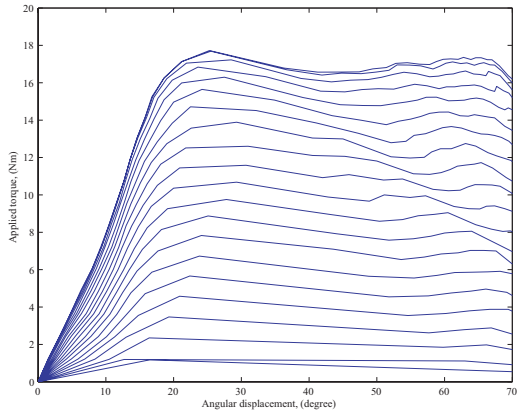

Fig. 5. Torque generated by the magnets as the angular displacement varies.

Using the parameters in Table II, an impact is simulated to calculate the HIC. It is assumed that the VSU is connected via ideal gears and the link is covered with non-rigid material, see Fig. 6. J_l represents the inertia of the link due to the gears. J_o is the inertia of the object that collides with the link. J_o is given as $M_o L^2$, where M_o is the mass of the object and L is the distance of the impact location from the joint. K_c is the stiffness of the cover. Note that the effect of the gear needs to be considered when J_l, J_o, and K_c are calculated. The HIC values are calculated with maximum and minimum stiffness. The calculated HIC is 119.58 with maximum stiffness and 31.77 with minimum stiffness.

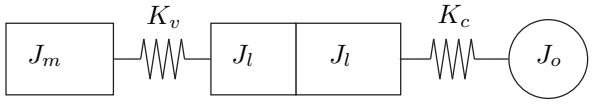

Fig. 6. Model of an impact to calculate the HIC. The link is assumed to be covered with non-rigid material.

The velocity of the link and the stiffness are shown in Fig. 7. The link is controlled to rotate at a given speed while stiffness is 20% of the maximum stiffness when the velocity is constant. When the link is rotating at a constant velocity,

Parameters	unit	Value	Parameters	unit	Value
J_l	(kgm^2)	5×10^{-4}	M_o	kgm^2	1×10^{-2}
K_c	(N/m)	1.5×10^2			

TABLE II

PARAMETERS FOR SIMULATION

the velocity is about $0.93rad/s$. During acceleration of the link, the stiffness changes from maximum to minimum while the stiffness increases from minimum to maximum when the link is decelerating.

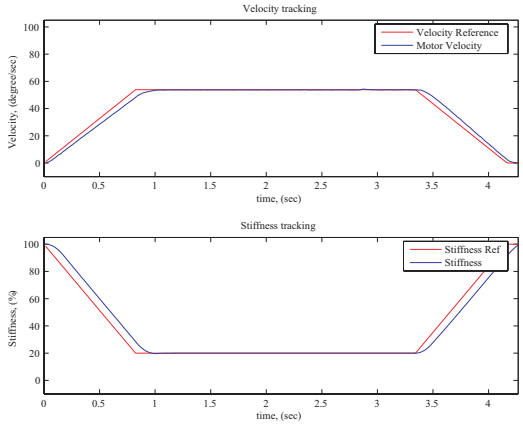

Fig. 7. Stiffness change while the joint follows trapezoidal velocity command. At constant velocity, the HIC remains less than 100.

V. CONTROL

In this section, control methodology is explained. Assuming the joint motor and the frame have a rigid connection and no friction exists between the link and the frame, the dynamics of the VSJ is given as follows.

$$\begin{aligned} J_l\ddot{q}_l + b_l\dot{q}_l + k(q_k)(q_l - q_m) &= 0 \\ J_m\ddot{q}_m + k(q_k)(q_m - q_l) &= u_m \\ J_k\ddot{q}_k &= u_k, \end{aligned} \tag{4}$$

where J_l is the inertia of the rotor and the link, J_m is the inertia of the stator and the frame, J_k is the inertia of the mechanism to change the stiffness including the lead screw and the nut, b_l is the damping coefficient of the link, u is the torque, and the stiffness generated by the VSU is represented by $k(q_k)$. q_l is the angle of the link, q_m is the angle of the joint motor, q_k is the angle of the VSU motor, see Fig. 8. Since the translational movement of the stator is resulted from the VSU motor and the stiffness is proportional to the height of the overlapping area, $k(q_k) = \alpha q_k$, where α is a constant.

Let $\mathcal{Q}$ be an open subset of $\mathbb{R}^3$ and $x = (q_l, q_m, q_k, \dot{q}_l, \dot{q}_m, \dot{q}_k)' \in \mathcal{TQ}$. Then, the dynamics in the state-space becomes

$$\dot{x} = f(x) + g_m(x)u_m + g_k(x)u_k, \tag{5}$$

where u_m represents the torque applied to the joint motor and u_k denotes the torque applied to the VSU motor. Let

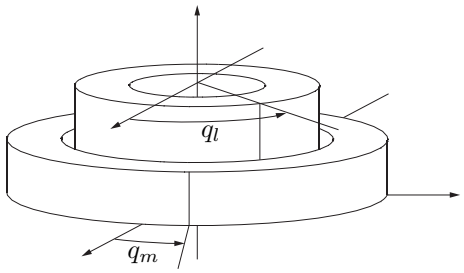

Fig. 8. State definition. q_k is not shown in the figure. Since the stator is moved using the VSU motor, the translational displacement is proportional to the angle of the VSU motor.

$y = h(x) = (h_1(x), h_2(x))' = (q_l, q_k)'$ be a 2×1 vector of output functions. Differentiating the output function $h_1(x)$ four times yields

$$\frac{\partial^4 h(x)}{\partial x^4} = L_f^4 h_1(x) + L_{g_m} L_f^3 h_1(x) u_m + L g_k L_f^3 h_1(x) u_k, \tag{6}$$

where $L_{g_m} L_f^3 h_1(x) \neq 0$ and $L_{g_k} L_f^3 h_1(x) \neq 0$. Since $L_{g_m} L f^n h_1(x) = L_{g_k} L_f^n h_1(x) = 0$ for $n = 0, 1, 2$, the relative degree with the output function $h_1(x)$ is 4. Similarly, differentiating the output function $h_2(x)$ twice gives

$$\frac{\partial^2 h_2(x)}{\partial x^2} = L_f^2 h_1(x) + L g_k L_f h_2(x), \tag{7}$$

where $L g_k L_f h_2(x) \neq 0$, which implies the relative degree of the output function $h_2(x)$ is 2. Therefore, the relative degree of the system is $(4, 2)$. Since $L g_m L_f^3 h_1(x) \neq 0$ and $L g_k L_f^3 h_1(x) \neq 0$, the decoupling matrix

$$A = \begin{bmatrix} L g_m L_f^3 h_1(x) & L g_k L_f^3 h_1(x) \\ 0 & L g_k L_f^2 h_2(x) \end{bmatrix} \tag{8}$$

is invertible. Therefore, control input

$$u = \begin{bmatrix} u_m \\ u_k \end{bmatrix} = -A^{-1} \left(\begin{bmatrix} L_f^4 h_1(x) \\ L_f^2 h_2(x) \end{bmatrix} - \nu \right) \tag{9}$$

is feedback linearizing control for the system.

Since $L f^i h_1(x)$ for $i = 0, 1, 2, 3$ and $L f^j h_2(x)$ for $j = 0, 1$ are linearly independent [18], coordinate transformation

$$z = \Phi(x) = \begin{bmatrix} h_1(x) \\ L_f h_1(x) \\ L_f^2 h_1(x) \\ L_f^3 h_1(x) \\ h_2(x) \\ L_f h_2(x) \end{bmatrix} \tag{10}$$

is valid. Then, the system is feedback linearized with the control (9) to yield

$$\begin{cases} \dot{z} = Az + B\nu \\ y = Cz \end{cases} \tag{11}$$

where

$$A = \begin{bmatrix} 0 & 1 & 0 & 0 & 0 & 0 \\ 0 & 0 & 1 & 0 & 0 & 0 \\ 0 & 0 & 0 & 1 & 0 & 0 \\ 0 & 0 & 0 & 0 & 0 & 0 \\ 0 & 0 & 0 & 0 & 0 & 1 \\ 0 & 0 & 0 & 0 & 0 & 0 \end{bmatrix} \quad B = \begin{bmatrix} 0 & 0 \\ 0 & 0 \\ 0 & 0 \\ 1 & 0 \\ 0 & 0 \\ 0 & 1 \end{bmatrix} \quad (12)$$

$$C = \begin{bmatrix} 1 & 0 & 0 & 0 & 0 & 0 \\ 0 & 0 & 0 & 0 & 1 & 0 \end{bmatrix}$$

Since the system (11) is controllable, it is possible for the feedback gain K is determined to place the poles of the system at a desired location. Let K be stabilizing feedback gain of (11). Then, $\nu = -Kz + \mu$ yields

$$\dot{z} = (A - KB)z + B\mu = \bar{A}z + B\mu \quad (13)$$

$$y = Cz, \quad (14)$$

where $\bar{A}$ is Hurwitz.

Fig. 10 is experimental result of the VSU tracking a step reference. A step reference is applied for the link to track while the stiffness of the VSJ remains at the maximum. Due to the friction that is not modeled in (4), there is steady state error.

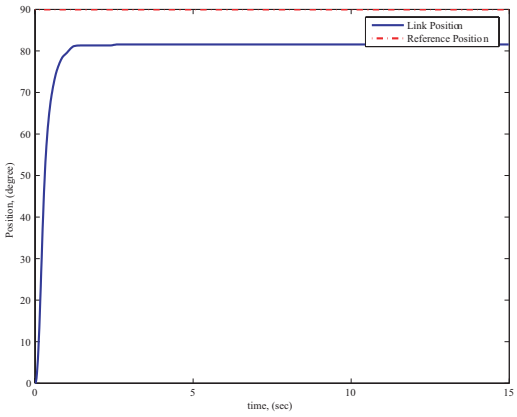

Fig. 9. Step response of the VSJ with feedback linearizing controller. Steady state error exists due to model uncertainty and disturbances.

In order to reduce the error caused by model uncertainty and disturbances, an integral controller is introduced. Let $\bar{z} = (z, w)'$ be a state vector for the augmented system, which is given as follows

$$\dot{\bar{z}} = \begin{bmatrix} A & 0 \\ a & 0 \end{bmatrix} \bar{z} + \begin{bmatrix} B \\ 0 \end{bmatrix} \nu \quad (15)$$

$$y = \begin{bmatrix} C & 0 \end{bmatrix} \bar{z}, \quad (16)$$

where $a = \begin{bmatrix} 1 & 0 & 0 & 0 \end{bmatrix}$. Then, $\nu = -\begin{bmatrix} K & k_I \end{bmatrix} \bar{z} + \mu$ is stabilizing controller for the augmented system (16).

Note that motor and states saturation need to be considered when determining the stabilizing control gain for experimental setup. In reality, the torque generated by each motor and the angles of the link and the VSU motor are allowed within certain boundary. In designing control gain, required torque and angles of the link and the VSU motor need to be checked if the boundary constraints are satisfied.

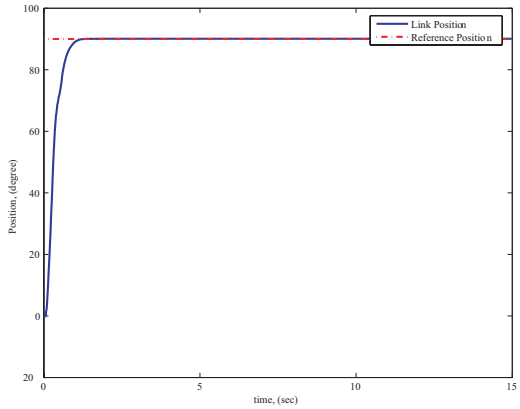

Fig. 10. Step response of the VSJ with integral controller.

VI. CONCLUSIONS

A robot joint with variable stiffness unit (VSU) was presented. The VSU utilized permanent magnets to generate torque. The magnets formed two concentric rings and generated torque when relative angular displacement occurs. The torque generated by the magnets was varied as the overlapping area changed. The overlapping area was changed by the translational displacement of the stator, which resulted in changing stiffness for the same angular displacement. The implemented VSU was capable of reducing the stiffness to almost zero, which ensured safety at wide range of operating speed. Feedback linearization methods was used to control the position and the stiffness of the VSJ. In addition to the feedback linearizing control, integral control was augmented to reject steady state error caused by model uncertainties and disturbances.

REFERENCES

[1] B. R. Shetty and M. H. Ang Jr., "Active compliance control of a PUMA 560 robot," in *Proc. of the 1996 IEEE International Conference on Robotics and Automation, Minneapolis, MN.*, April 1996, pp. 3720–3725.

[2] M. Zinn, B. Roth, O. Khatib, and J. K. Salisbury, "A new actuation approach for human friendly robot design," *International Journal of Robotics Research*, vol. 34, no. 4–5, pp. 379–398, April–May 2004.

[3] W. Wang, R. N. K. Loh, and E. Y. Gu, "Passive compliance versus active compliance in robot-based automated assembly systems," *Industrial Robot*, vol. 25, no. 1, pp. 48–57, 1998.

[4] A. Bicchi, S. L. Rizzini, and G. Tonietti, "Compliant design for intrinsic safety: General issues and preliminary design," in *Proceedings of the 2001 IEEE/RSJ Conference On Intelligent Systems and Robots, Maui, Hawaii*, April 2004, pp. 249–254.

[5] G. Tonietti, R. Schiavi, and A. Bicchi, "Design and control of a variable stiffness actuator for safe and fast physical human/robot interaction," in *Proc. of the 2005 IEEE International Conference on Robotics and Automation, Barcelona, Spain*, April 2005, pp. 526–531.

[6] T. Morita and S. Sugano, "Design and development of a new robot joint using a mechanical impedance adjuster," in *Proc. of the 1995 IEEE International Conference on Robotics and Automation, Nagoya, Japan*, May 1995, pp. 2469–2475.

[7] M. Okada, Y. Nakamura, and S. Ban, "Design of programmable passive compliance shoulder mechanism," in *Proc. of the 2001 IEEE International Conference on Robotics and Automation, Seoul, Korea*, May 2001, pp. 348–353.

[8] M. Okada and Y. Nakamura, "Development of a cybernetic shoulder - a 3-dof mechanism that imitates biological shoulder motion," *IEEE Transactions on Robotics*, vol. 21, no. 3, pp. 438–444, 2005.

[9] S.-S. Yoon, S. Kang, S.-J. Kim, Y. Kim, M. Kim, and C. Lee, "Safe arm with mr-based passive compliant joints and visco-elastic covering for service robot application," in *Proceedings of the 2003 IEEE/RSJ Conference On Intelligent Systems and Robots, Las Vegas, Nevada*, October 2003, pp. 2191–2196.

[10] M. W. Spong, "Modeling and control of elastic joint robots," *Journal of Dynamic Systems, Measurement, and Control*, vol. 109, pp. 310–319, December 1987.

[11] A. De Luca, "Dynamic control of robots with joint elasticity," in *Proceedings of the IEEE International Conference On Robotics and Automation*, Philadelphia, Pennsylvania, April 1988, pp. 152–158.

[12] A. De Luca and P. Lucibello, "A general algorithm for dynamic feedback linearization of robots with elastic joints," in *Proc. of the 1998 IEEE International Conference on Robotics and Automation, Leuven, Belgium*, May 1998, pp. 504–510.

[13] J. Versace, "A review of the severity index," in *Proc. of the 15th Stapp Car Crash Conference*, 1971, pp. 771–796.

[14] R. M. Hornreich and S. Shtrikman, "Optimal design of synchronous torque couplers," *IEEE Transaction on Magnetics*, vol. MAG-14, no. 5, pp. 800–802, September 1978.

[15] M. Zinn and O. Khatib, "Playing it safe," *IEEE Robotics & Automation Magazine*, pp. 12–21, June 2004.

[16] A. Bicchi and G. Tonietti, "Fast and "soft-arm" tactics," *IEEE Robotics & Automation Magazine*, pp. 22–33, June 2004.

[17] NHTSA, "Actions to reduce the adverse effects of air bags FMVSS No. 208," February 1997.

[18] A. Isidori, *Nonlinear Control Systems*, 3rd ed. Springer, 2001.